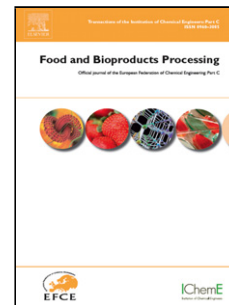


## Accepted Manuscript

Title: Effect of type of encapsulating agent on physical properties of edible films based on alginate and thyme oil

Author: Rosa Navarro Carla Arancibia María Lidia Herrera  
Silvia Matiacevich



PII: S0960-3085(15)00137-6  
DOI: <http://dx.doi.org/doi:10.1016/j.fbp.2015.11.001>  
Reference: FBP 656

To appear in: *Food and Bioproducts Processing*

Received date: 3-7-2015  
Revised date: 16-10-2015  
Accepted date: 23-11-2015

Please cite this article as: Navarro, R., Arancibia, C., Herrera, M.L., Matiacevich, S., Effect of type of encapsulating agent on physical properties of edible films based on alginate and thyme oil, *Food and Bioproducts Processing* (2015), <http://dx.doi.org/10.1016/j.fbp.2015.11.001>

This is a PDF file of an unedited manuscript that has been accepted for publication. As a service to our customers we are providing this early version of the manuscript. The manuscript will undergo copyediting, typesetting, and review of the resulting proof before it is published in its final form. Please note that during the production process errors may be discovered which could affect the content, and all legal disclaimers that apply to the journal pertain.

**Highlights**

Trehalose,  $\beta$ -cyclodextrin and Tween 20 allow obtaining emulsion forming films.

Tween 20 film has the highest opacity which can affect the organoleptic characteristics of a product.

$\beta$ -cyclodextrin films have crystals that may change its properties with time.

Accepted Manuscript

**Effect of type of encapsulating agent on physical properties of edible films based on alginate and thyme oil**

**Rosa Navarro<sup>1</sup>, Carla Arancibia<sup>1</sup>, María Lidia Herrera<sup>2</sup> and Silvia Maticceich<sup>1\*</sup>**

*<sup>1</sup>Food Properties Research Group, Departamento de Ciencia y Tecnología de los Alimentos, Facultad Tecnológica, Universidad de Santiago de Chile. Obispo Umaña 050, Estación Central, Santiago, Chile.*

*<sup>2</sup>Instituto de Tecnología en Polímeros y Nanotecnología ITPN (UBA-CONICET) Facultad de Ingeniería, Universidad de Buenos Aires, Av. Las Heras 2214, C1127AAQ, Ciudad Autónoma de Buenos Aires, Argentina.*

*<sup>1</sup>Corresponding author*

Silvia Maticceich

Phone: +56 2 227184517

e-mail: [silvia.maticceich@usach.cl](mailto:silvia.maticceich@usach.cl)

**Abstract**

Active edible coatings incorporating antimicrobial agents such as thyme oil are studied to improve the shelf-life of fresh foods. The type of encapsulating agents used to microencapsulate the active compound could affect both, emulsions and film's physical properties. The aim was to study the effect of different encapsulating agents (trehalose,  $\beta$ -cyclodextrin and Tween 20) on physical and antimicrobial properties of alginate/thyme oil emulsions and films. Physical and antimicrobial characterization of film-forming emulsion and films were developed. Results showed differences in rheological behavior, particle size and stability of emulsions by encapsulating type. The highest stability of emulsions containing Tween 20 (instability of 0.69%) was attributed to more interactions between components (observed by FTIR) and the lowest particle size, but other samples also showed high stability (instability <5%). The stability of emulsions did not correlate with films microstructure indicating that interactions amount components changed when solvent was evaporated. Films containing trehalose and  $\beta$ -cyclodextrin had less color and opacity than Tween 20, which is an advantage by industrial applications by coating due cannot affect the organoleptic characteristics of a fresh product. In conclusion, it is important the choice of encapsulating agent in order to use for developing active coatings with potential for applications in fresh food.

**Keywords:** alginate, thyme oil, encapsulating agents, films, emulsions, physical properties

## 1. Introduction

Food quality and safety are the major concerns in the food industry, especially on preventing chemical and microbiological deterioration, as well as the exposure of labile biomolecules (vitamins, essential oils, colorants) to extreme humidity and temperature conditions, which leads them to degradation (Ponce Cevallos et al. 2010). For this, the interest in development of novel ways to prolong the shelf life of food products has increased in the last years. Edible films as a solid sheet can be applied on the surface of the food systems and can be a good alternative to improve food quality by serving as selective barriers to moisture transfer, carbon dioxide permeability, oxygen uptake, lipid oxidation, and losses of volatile aromas and flavors (Kester and Fennema 1986; Di Piero et al. 2011; Lacroix and Vu 2014).

These films are thin layers of edible material such as protein, polysaccharide and lipid. Among polysaccharides, alginate, is widely used to produce films (Rojas-Grau et al. 2007; Córdova et al. 2015), which can be used to carry active ingredients, for example antioxidant and antimicrobial agents (Tapia et al. 2008). Studies have focused on the incorporation of natural active compounds in edible film since they may widen the functionality protecting the product from microbial spoilage and thus extend their shelf-life (Mchugh and Senesi 2000; Alboofetileh et al. 2014; Karagöz et al. 2010; Peretto et al. 2014).

Essential oils and their constituents have been frequently used as flavors agents in foods and are categorized as Generally Recognized as Safe (GRAS) (López et al. 2007; Hill et al. 2013). Essential oils rich in phenolic compounds have been reported to have a wide spectrum of antimicrobial activity. Among these, clove, oregano, rosemary, sage vanillin and oils have been found to be effective antimicrobial agent (Holley and Patel 2004; Burt 2004), specifically thyme and oregano essential oils have been pointed out to possess better antimicrobial potential for meat applications because carvacrol, thymol, c-therpinene and p-cymene are the principal constituents of oregano and thyme essential oils (Burt, 2004; Solomakos et al. 2008). However these compounds are highly volatile, insoluble in water due to their lipophilic nature and may suffer degradation reactions in the presence of ambient oxygen and light as well as under the action of moderate temperatures (Beyki et al. 2014).

One way to allow their incorporation into matrices is through an encapsulation process which can be classified as: physical-chemical processes (coacervation, emulsion evaporation), chemical processes (gelling, complexation) and physical processes (fluidized bed, extrusion, spray drying, spray cooling), where the emulsion evaporation has been used as release system for a lot of ingredients and functional foods and is probably the release of lipids system most used in the food industry (Esparza and Irache,

2011). For the preparation of emulsion is possible to use different encapsulating agents such as cyclodextrins, tween 80 and 20, trehalose, maltodextrin, pectin, capsul (Drusch et al. 2006; Álvarez-Cerimedo et al. 2008; Ponce Cevallos et al. 2010; Karunasawat and Anprung 2010; Aguiar et al. 2012; Hill et al. 2013), due to their ability to facilitate the formation, improve the stability, and produce desirable physicochemical properties in oil-in-water emulsions.

Cyclodextrins are cyclic oligosaccharides where the central cavity is hydrophobic, while the rims of the surrounding walls are hydrophilic (Del Valle 2004; Gibara et al. 2015). However, much of the interest in cyclodextrin arises precisely from their ability to encapsulate hydrophobic molecules with suitable size inside their annulus to form inclusion complexes and then to alter physical, chemical, and biological properties of the encapsulated guest molecules (Ponce Cevallos et al. 2010). In the same way, trehalose appears to be very promising for microencapsulation because it possesses a uniquely high glass transition temperature and remains in the glassy state at temperatures higher than other sugars and has a greater capability of stabilizing proteins, lipids or carbohydrates (Drusch et al. 2006). Besides, it has been reported that edible hydrocolloid films prepared with trehalose could act as very effective barriers to gases, especially to CO<sub>2</sub>, showing a higher barrier compared to similar films obtained with glycerol as plasticizer (Giosafatto et al. 2014).

Drusch et al. (2006) who used 10% trehalose concentration, reported that encapsulation in a trehalose matrix offers protection for the microencapsulated fish oil for a certain period of time and Hill et al. (2013) utilized beta- cyclodextrin to encapsulate different essential oils (trans-cinnamaldehyde, eugenol, cinnamon bark, and clove bud extracts) mixed in an aqueous solution in a 1:1 molecular ratio. He reported that such essential oil inclusion complexes could be useful antimicrobial delivery systems with a broad spectrum of application in food systems where Gram-positive and negative bacteria could grow.

Little work has been done on the effect of encapsulating agent on physical properties of films. However, the type of encapsulating molecules could affect both, emulsions and film physical properties. The aim of the present work was to study the effect of different encapsulating agents on physical properties of alginate/thyme oil emulsions and films. Both systems were investigated in order to obtain information that can be used for developing coatings with potential for applications in fresh food.

## **2. Materials and Methods**

### **2.1 Composition and preparation of samples**

Thyme oil was purchased from commercial local company (Ambar, Santiago, Chile); Sodium alginate (G5706401), trehalose dihydrate [D-glucopyranosyl-(1-1)-Dglucopyranoside] (S-518) and sorbitol (20/60 DC) were provided by Blumos S.A. (Santiago, Chile); calcium carbonate was purchased from Winkler Ltda. (Santiago, Chile);  $\beta$ -cyclodextrin and Tween 20 were obtained from Merck S.A. and Sigma Aldrich Co. (Santiago, Chile), respectively. All reagents were used without any further purification.

Film-forming emulsions were prepared by mixing 100 g of aqueous phase and 0.5 % (wt/wt) of thyme oil phase. In all cases, aqueous phase was prepared with sodium alginate 1% (wt/wt), sorbitol 1% (wt/wt) and calcium carbonate 0.02% (wt/wt). Three different encapsulating agents were used: trehalose (0.2; 0.4; 0.6 and 0.8 % wt/wt),  $\beta$ -cyclodextrin (0.1; 0.15; 0.2 and 0.25%wt/wt), and Tween 20 (1; 1.5; 2 and 2.5 % wt/wt). Emulsions were prepared by magnetic stirred moderately at 40 °C until the solutes were completely dissolved. Then, thyme oil was incorporated using an homogenizer (Trhistor Regler TR50, Germany) at 5000 rpm for 1 min. Films were obtained from film-forming emulsions by casting method at 40°C for 20 h in forced air oven (Wiseven DaihanScientific WOF-105, Korea). Film control with thyme oil was prepared without any encapsulating agent. Films were stored in desiccators for 24 h prior to analysis.

## 2.2 Film-forming emulsion characterization

### 2.2.1 Flow behavior

Flow measurements were carried out in a controlled stress rheometer (CarriMed, CSL2 100, TA Instruments, UK), using parallel-plate geometry (40 mm diameter; 1.5 mm gap). Measurements were run at 25±1°C and after loading the sample, it was allowed to stand for 3 min to stabilize and reach the desired temperature. At least two batches of each composition were prepared and each batch was measured in triplicate, using a fresh sample for each measurement.

Curve flows were obtained by recording shear stress values, which was increased from 0 to 250 Pa and decreased from 250 to 0 in 240 s. Experimental data from ascending flow curves of film-forming emulsions were fitted to the Ostwald-de Waele model (Eq. 1).

$$\sigma = K \dot{\gamma}^n \quad (\text{Eq. 1})$$

where  $\sigma$  (Pa) is the shear stress,  $K$  (Pa s<sup>n</sup>) is the consistency index,  $\dot{\gamma}$  (s<sup>-1</sup>) is the shear rate,  $n$  is the flow index, and  $\sigma_0$  (Pa) is the yield stress.

### 2.2.2 Particle size and distribution

The average particle size and size distribution were measured by Dynamic Light Scattering using a Zetasizer Nano S (Malvern Instruments, UK). The film-forming emulsions were diluted with deionized water to 1/10 of their original concentrations. A refractive index value of 1.47 was used for the disperse phase (Thyme oil) and of 1.33 for the continuous phase (water) (Bonilla et al. 2012). The particle size of samples was described by the cumulants mean (Z-average) diameter and the size distribution was described by the polydispersity index (PDI) and the size distribution graph. Measurements were made in triplicate for each film-forming emulsion.

### 2.2.3 Stability

The emulsion stability was analyzed using a vertical scan analyzer (Turbiscan MA 2000, Formulation, France). The reading head is composed of a pulsed near-IR light source ( $\lambda = 850$  nm) and two synchronous detectors. The transmission detector receives the light, which goes through the sample ( $0^\circ$ ), while the back-scattering detector receives the light back-scattered (BS) by the sample ( $135^\circ$ ). Samples were put in a cylindrical glass measurement cell and the backscattering (BS) profiles as a function of the sample height (total height = 60 mm) were studied in quiescent conditions at  $22.5 \pm 0.5$  °C. In this way, the BS evolution is followed without disturbing the original system and with good accuracy and reproducibility (Mengual et al. 1999; Cerdeira et al. 2007). Measurements were performed immediately after preparation of the samples by triplicate and during storage time at  $40^\circ\text{C}$ , which is the temperature of the casting method used.

## 2.3 Film characterization

### 2.3.1 Optical characterization (color difference and opacity)

Digital images from each film (white and black background) were captured through a computer vision system, which consisting of a black box with four natural daylight (D65) (18W, Philips) and a digital camera (Canon Powershot G3 14 MP, Japan) at a distance of 22.5 cm from sample (camera lens angle and light at  $45^\circ$ ) (Pedreschi et al. 2006). All images were acquired at the same conditions and the camera was remotely controlled by EOS Utility software (Canon, USA). Images were analyzed extracting color values in RGB (red, green and blue) space using Adobe Photoshop v7.0 program (Adobe Systems Incorporated, USA), and then converted to CIEL\*a\*b\* space, where L\* is black-white component



(lightness),  $a^*$  is red-green component and  $b^*$  is yellow-blue component. The variation of colour between each sample and the control (without encapsulating agent) were calculated using CIE $\Delta E_{2000}$  equation (Luo et al. 2001). A color difference (CIE $\Delta E_{2000}$ ) value higher than 12 indicates a subjective assessment of “very much” perception of color differences (Yang et al. 2012).

The opacity of the film was obtained using the values of lightness ( $L^*$ ) obtained from the films using white ( $L^*$ white) and black ( $L^*$ black) background (Eq. 2), where a value of 100% indicates a film opaque and a value of 0% indicates a transparent film.

$$\% \text{ Opacity} = (L^* \text{ black}) / (L^* \text{ white}) * 100 \quad (\text{Eq. 2})$$

Data reported were the average of five films of each sample with their corresponding standard deviation.

### 2.3.2 Molecular mobility by NMR

A pulsed nuclear magnetic resonance ( $^1\text{H}$  NMR) Bruker Minispec spectrometer model mq 20 (Bruker Biospin GmbH, Germany) with a 0.47 T magnetic field operating at resonance frequency of 20 MHz and thermo stated at 40 °C, was used for the measurements. The technique ( $^1\text{H}$  NMR), measuring the half-life spin-spin transverse relaxation times ( $T_2$ ), was used to determine water and solid mobility following the method described by Farroni et al. (2008). The emission signal spin-spin relaxation times called free induction decay (FID) is recorded by the instrument as the nuclei magnetic moments relax back to equilibrium with the applied magnetic field. FID analysis was used to evaluate proton mobility associated with the matrix in the range 4-90°C (Roudaut et al. 1998; Farroni et al. 2008). The samples were placed in 10 mm diameter glass tubes (to 5 cm height) and equilibrated at different temperatures (from 5.0 to 90.0°C) in a thermostatted bath (Thermo Haake C35P, Germany) before measuring  $T_{2\text{FID}}$ . The FID test itself is very fast, taking lower than 10 s, and samples could be measured without appreciable temperature modification during test. The decay envelopes were fitted to monoexponential behavior with the following equation:

$$I = A e^{-t/T_{2\text{FID}}} \quad (\text{Eq. 3})$$

where  $I$  represents proton signal intensity,  $T_{2\text{FID}}$  corresponds to the relaxation time of protons in the polymeric chains of the sample and tightly bound water, and  $A$  is a constant.

### 2.3.3 Fourier-transform infrared (FTIR) spectroscopy

The infrared spectra of films were recorded using a Fourier-transformed infrared spectrophotometer (Spectrum Two, Perkin-Elmer System, USA). The analysis was performed using an attenuated total reflectance (ATR) cell, in a spectral range of 4000-400  $\text{cm}^{-1}$  at a resolution of 4  $\text{cm}^{-1}$ . At least three replicates were run for each film.

#### **2.3.4 Microstructure by scanning electron microscopy**

Scanning electron microscopy (SEM) was used to analyze the surface and cross-sections of the films. Dried samples (5x3 mm) were mounted on specimen stubs. After that, they were freeze-dried, sputter-coated (Cressington Scientific Instruments, 108 Sputter Water, Germany) with platinum and examined using a scanning electron microscope (Supra 40, Carl Zeiss NTS, Oberkochen, Germany) at 3 kV. For cross-section observation, the samples were previously fractured using liquid nitrogen.

#### **2.3.5 Differential scanning calorimetry (DSC)**

DSC was used to determine encapsulation efficiency of thyme oil in different films. The methodology used was described in Ponce Cevallos et al. (2010). Briefly: encapsulation percentage of thyme oil was determined as 100 minus the ratio (expressed in percentage) of the fusion enthalpies of films and of the pure compound. The heat of fusion defined as the change in enthalpy ( $\Delta H$ ) was calculated from the area under their corresponding endothermic peak. Films were measured immediately after preparation. Analysis was performed using a Mettler Toledo instrument model DSC F822e (Mettler Toledo, Switzerland). Samples of free thyme oil and films containing it were weighed ( $\pm 11$  mg) and placed into 40mL hermetically sealed aluminum pans. Samples were studied using a scanning rate of 10  $^{\circ}\text{C}/\text{min}$  from -35 to 70  $^{\circ}\text{C}$ , under a nitrogen atmosphere (ultra-pure). Prior the measurements, the DSC was calibrated using indium (melting onset temperature 156.6 $\pm$ 1.6 $^{\circ}\text{C}$ ,  $\Delta H = 28.6\pm 1$  J/g). The reference used during the analysis was an empty pan. Measurements were performed in duplicates following the same protocol. Efficiencies were expressed in dry basis and average and standard deviation were reported.

#### **2.3.6 Antimicrobial activity**

As described by Matiacevich et al. (2013), antimicrobial activity of the films was evaluated against *E. coli* (ATCC 25922), obtained from the ISP (Health Public Institute, Chile). Bacteria stored at -20 $^{\circ}\text{C}$  in Mueller Hinton broth with 20% w/w skim milk until use, was grown in Mueller Hinton broth (DIFCO,

France) at 37°C overnight. This culture served as the inoculums for the microbiological studies, these colony-forming units (CFU) counts were accurately and reproducibly obtained by absorbance value measured by optical density at 625 nm on a spectrophotometer (Shimadzu UVmini-1240, Japan), which corresponded to a 0.5 McFarland turbidity standard solution (approximately  $10^8$  CFU/ mL) (CDCP and WHO 2003) and diluted starting with a final concentration of each bacterium of  $1 \times 10^5$  (CFU)/mL. Films for antimicrobial activity were prepared immediately before using them. The antimicrobial activity of different concentrations of each encapsulating agent against *E. coli* was determined by the agar diffusion method, which consisted of placing a piece of film (1cm<sup>2</sup>) on Muller Hinton agar plates inoculated with *E. coli* ( $1 \times 10^5$  CFU/mL) and incubating at 37 ° C for 24 h. After the incubation time, the images were obtained using a digital camera (Canon Powershot G3 4MP, Japan) and the growth inhibition of the different films (zone below film) was determined comparing to the control zone (zone without films).

#### **2.4 Data analysis**

At least two batches of each composition were prepared and each batch was measured in triplicate for all measurements. An analysis of variance (ANOVA) of two factors (type and concentration of encapsulating agent) was performed to determine the effect of factors and their interaction on different parameter. Fisher's test with a 1% of significance level was used to determine the least significant difference between samples. All analyses were performed using the XLSTAT Pro software, version 2014 (Addinsoft, France).

### **3. Results and discussion**

#### **3.1 Film-forming emulsions**

##### **3.1.1 Flow behavior**

The flow curves of all film-forming emulsions showed a slight No-Newtonian and shear thinning behavior with *n* values from 0.86 to 0.90. In emulsions with low oil contents, the particles are far apart and the inter-particle interactions are relatively weaker (Zúñiga et al. 2012). This structural conformation explains the low consistency of these systems and their slight pseudoplasticity. A similar behavior was obtained by Ortega-Toro et al. (2014) when studied the incorporation of different type of surfactant on film-forming emulsion based on starch. Figure 1 shows, as an example, the flow curves of samples

containing the highest and the lowest concentrations of each encapsulating agent. The experimental data of ascending rheograms were successfully fitted to the Ostwald-de Waele model with  $R^2$  values between 0.98 and 0.99. Two-way ANOVA of flow parameters values showed that the effect of interaction between encapsulating agent type and concentration was significant ( $p < 0.05$ ) on flow index ( $n$ ) and consistency ( $K$ ) values (Table 1). This interaction indicated that the effect of concentration on flow parameters was different depending on encapsulating agent type. In general, it was observed that the increase in Tween 20 concentration had a significant effect ( $p < 0.01$ ) on  $n$  and  $K$  values of emulsions and those containing 2% Tween 20 presented the highest consistency and pseudoplasticity (Table 2), due probably to the higher encapsulating agent viscosity, which increased the viscosity of the system. In the case of samples with  $\beta$ -cyclodextrin and trehalose, the concentration did not have a significant effect ( $p > 0.05$ ) on  $n$  and  $K$  values. These results indicate that the incorporation of  $\beta$ -cyclodextrin and trehalose at the concentrations studied did not promote notable changes in the flow behavior in the range of the shear rate analyzed and could point out that lower interactions between components occurred in these systems, comparing to Tween20. Similar results were obtained by Zúñiga et al. (2012) when sodium dodecyl sulfate (SDS) was added to the film-forming emulsion based on hydroxypropyl methylcellulose. On the other hand, the difference detected among the encapsulating agents on flow parameter values could be due to the amount or viscosity of surfactant added to the emulsions, which was greater in samples with Tween 20, promoting a significant increase of consistency ( $K$ ) and pseudoplasticity ( $n$ ) (Table 2).

### 3.1.2 Particle size

Figure 2 shows the droplet size distribution of different film-forming emulsions based on volume percent of droplets as a function of Z-average size. All samples presented a monomodal distribution and extended from 800 and 4500 nm. The average particle size of different samples were ranged between 2066 and 3536 nm, depending of the composition and the polydispersity indices (PDI) were obtained in the range of 0.23-0.51, showing a Gaussian particle size distribution. The PDI values measures the spread of the particle size distribution, and a PDI value  $> 0.7$  indicates that sample has a very broad size distribution. PDI values were not significantly ( $p < 0.05$ ) influenced by encapsulating agent type and concentration factors studied. ANOVA results showed that only encapsulating agent concentration had a significant effect on Z-average size values ( $F = 5.89$ ,  $p < 0.01$ ). In general, all samples with encapsulating agent presented lower particle size values than the control samples (without encapsulating agent). This result can be

attributed to the decrease of the interfacial tension between the oil and the aqueous phases by the surfactant addition because it reduces the amount of free energy required to deform and disrupt the droplets resulting in smaller droplets after homogenization process (McClements, 2005). Similar results were obtained by Zúñiga et al. (2012) when added sodium dodecyl sulphate (SDS) as surfactant in film-forming emulsions. In the samples with trehalose, the particle size decreased with increasing trehalose concentration and the emulsion with 0.8% trehalose exhibited the lowest Z-average size ( $2066\pm 192$  nm) and also was very homogenous ( $PdI:0.23\pm 0.11$ ). This is because smaller particles meant greater surface areas which would require more emulsifiers to cover the oil droplets (McClements, 2005; Yuan et al. 2008). Respect to the samples with  $\beta$ -cyclodextrin, it was not observed a clear trend with increasing concentration of encapsulating agent. Samples with the lowest  $\beta$ -cyclodextrin concentration presented the smallest particle size and one of the narrowest ranges of size distribution (Figure 2a, Table 4). Meanwhile with Tween 20, smaller particle size were observed at the lowest concentrations than those with the highest concentrations, although this difference in particle size was not significant ( $p<0.05$ ). This can be due to an excess of surfactant in the system. At the highest encapsulating concentrations there was more emulsifier than required to cover all droplets, so the particle size depended mainly of the maximum disruptive forces that can be generated within the homogenizer, which could be insufficient to get particle of lower size (McClements, 2005; Qian and McClements, 2011).

### 3.1.3 Physical stability by multiple light scattering (MLS)

The mechanisms involved in instability process of emulsions were studied as a function of storage time at  $40^{\circ}\text{C}$  in order to conduct the test in normal stresses for casting method conditions. Figure 3 shows back scattering profiles (%) along the tube length for film-forming emulsions formulated with the different encapsulating agents. Differences in instability process were observed depending of type of encapsulating agent used, being all samples stable until 48 h. After 72 h, most of the emulsions presented some phenomenon of instability. For samples with 0.8% trehalose (Figure 3a), a variation of the percentage of backscattering during time was observed, which was attributed to an increase in droplet size by coalescence or flocculation process, according to the theory of light scattering multiple (Mengual et al. 1999) and after 72 h of storage time, one peak was observed in the top of the tube, which indicates gravitational phase separation of the emulsion by creaming. Samples with 0.2%  $\beta$ -cyclodextrin (Figure 3b), showed an increase particularly pronounced at the bottom of the tube at 48 hours, which may be

explained by particles migration phenomena (sedimentation), indicating a complete destabilization of emulsions. Finally, the samples with Tween20 showed good stability, since no phenomena of kinetic instability of emulsions were observed, principally by coalescence of droplets (Figure 3c).

In order to evaluate quantitatively the influence of types of encapsulating agent on the stability of each emulsion, average variation of central-zone backscattering (30-32 mm of sample height) with storage time was analyzed. The average value (% BS) was plotted as a function of storage time (Figure 4).

The results, shown in Fig.4, were fitted to an exponential equation, generally used for a first order kinetic model (equation 4).

$$BS = BS_e + (BS_0 - BS_e)e^{(-k \cdot t)} \quad (\text{Eq. 4})$$

Where BS is the backscattering percentage as a function of storage time,  $BS_e$  corresponding to the backscattering percentage at the equilibrium value,  $BS_0$  is the initial value of backscattering, and K is the first-order kinetic coefficient.

The % BS light fluxes measured depend on the mean path length of photons (Mengual et al. 1999), and therefore progressive fall of % BS was observed on the whole height of the sample during storage time and can be related to droplet size increase (flocculation or coalescence). Emulsions stabilized with the different agent encapsulating, especially those samples that contained  $\beta$ -cyclodextrin agent, this phenomenon was much steep compared to the other samples (Figure 4 and Table 4).

The fitting parameters (Table 4) show that addition of Tween20 and trehalose stabilized the emulsions since these systems possessed kinetic coefficients of the instability process lower than the  $\beta$ -cyclodextrin agent. However, the emulsion with Tween20 although it proved to be the most stable, showed the highest value of K. Its %  $\Delta$  BS (the difference between BS and  $BS_0$ ) was just a 0.69 % indicating a stable system but the destabilization rate to the final BS was the fastest of the three emulsions. Respect to samples containing  $\beta$ -cyclodextrin, it is possible to observe instability phenomena with storage time, which presented a slope value much less steep compared to the other samples, especially at higher  $\beta$ -cyclodextrin concentrations. The K values decreased with the increase of encapsulating agent concentration, showing that  $\beta$ -cyclodextrin was efficient slowing destabilization phenomenon. The emulsion with 0.25 w/w %  $\beta$ -cyclodextrin had a %  $\Delta$  BS of 1.18% and a slower destabilization rate as indicated by parameter K value. These results are consistent with the reported by Drusch et al. (2006) where data clearly show that encapsulation in a trehalose matrix offers protection for the encapsulated oil for a certain period of time. In addition, Álvarez-Cerimedo et al. (2008) described that trehalose-sodium

caseinate matrix was the most effective for encapsulating a blend of sunflower oil in a high-melting fraction of milk fat. Finally the  $\beta$ -cyclodextrin proved to have a poor effect on their role as a stabilizer at high concentration, for this type of emulsion. The results obtained in this study indicate the importance of the choice of encapsulating agent and how the physical properties could be affected by the incorporation of antimicrobial (thyme) in emulsion.

It was reported that emulsion stability was a key property that influenced dehydrated powders physical properties (Álvarez-Cerimedo et al. 2008). It may be expected that it also affects the functionality of films for protecting food products especially regarding fruit coating by spraying, for example.

### 3.2 Edible films

#### 3.2.1 Color and opacity

A two-way ANOVA with interaction was applied to color difference (CIEDE2000 or  $\Delta E_{2000}$ ) and opacity parameters (Table 5). Results showed that the encapsulating agent type and concentration, as well as their interaction, had a significant effect ( $p < 0.01$ ) on  $\Delta E_{2000}$  and opacity values. This interaction indicated that concentration effect was different depending on encapsulating agent type. All films showed  $\Delta E_{2000}$  values over 1, being this variation noticeably perceptible by the human eye. Eye may distinguish color difference only if  $\Delta E_{2000}$  is greater than 1 (Yang et al. 2012). Samples with Tween 20 showed the greatest color difference (Figure 5a) and the film with 2% Tween20 showed the most appreciable color difference ( $\Delta E_{2000}$  values = 5.2).  $\beta$ -cyclodextrin concentration had a minor effect on color and  $\Delta E_{2000}$  values varied among 1.2 and 2.3.

With regard to the opacity parameter, results showed a clear effect of the concentration on opacity percentages and it was different for each encapsulating type. In all cases, the encapsulating agent addition increased significantly ( $p < 0.01$ ) the opacity of films. Samples with  $\beta$ -cyclodextrin and Tween 20 showed a increasing significant ( $p < 0.01$ ) of opacity values as increasing encapsulating concentration, being this variation was more noticeable in the films with Tween 20. At the highest concentrations of Tween 20 (1.5 and 2%), very opaque films (>60%) were obtained. In the case of samples containing trehalose, the opacity values almost did not varied with the concentration (Figure 5b), obtaining films almost transparent. These differences on optical properties of the films can be related with their internal structure developed during the film drying (Villalobos et al. 2005; Fabra et al. 2009). This structure is greatly affected by the initial structure of the emulsions (volume fraction of the dispersed lipids and size of lipid

aggregates) and their development throughout the drying process due to flocculation, coalescence and creaming. The effect of the size of lipid aggregates on optical properties, for a determined volume fraction of the dispersed phase, is difficult to predict due to the complexity of the interaction between particle size and light scattering (Birkett et al. 1985; Fabra et al. 2009).

### 3.2.2 Molecular mobility by Nuclear Magnetic Resonance Analysis

The study of  $^1\text{H}$  NMR spin-spin transverse relaxation times ( $T_{2\text{FID}}$ ) as a function of temperature and concentration of encapsulating agent provides information about the mobility of protons belonging to water and/or solids from the matrix, according to the pulse sequence employed (Farroni et al. 2008). Figure 3 shows the values of  $T_{2\text{FID}}$ , obtained by free induction decay analysis (single  $90^\circ$  pulse), for films with different concentrations of trehalose (a),  $\beta$ -cyclodextrin (b) and Tween20 (c) as a function of temperature. As expected,  $T_{2\text{FID}}$  value increased with the increase of temperature. According to Farroni et al. (2008) and Ritota et al. (2008) this increase reflects higher mobility of the protons in solids and water molecules. In addition, Chung et al. (2000) found that the changes in  $T_{2\text{FID}}$  versus temperature for several food powders were highly associated with physical changes, including agglomeration, water vaporization, and caking behavior. In general, according to the result of multifactor ANOVA, it is possible to observe that the relaxation time ( $T_{2\text{FID}}$ ), was dependent on the type of encapsulating agent and the temperature ( $p < 0.01$ ), however, there was no significant effect with concentration ( $p > 0.01$ ). The highest values of  $T_{2\text{FID}}$ , showing the overall increasing mobility in the matrix was observed in films containing Tween 20, while films with  $\beta$ -cyclodextrin showed the lowest values, where the lower mobility was attributed to crystallization or agglomeration of  $\beta$ -cyclodextrin into the matrix. This phenomenon, where the overall mobility in the matrix is reduced, could be associated to the increases of intermolecular forces between components (Fundo et al. 2014). Furthermore, the interaction between them gives rise to several structural changes in each region: fat crystals, air bubbles, surfactant micelles, and sugar crystal, which could also affect the molecular mobility. From NMR data, it could be expected that thyme release was slower for  $\beta$ -cyclodextrin films.

### 3.2.3 FTIR spectroscopy



FTIR spectra of films with different encapsulating agent are shown in Figure 7. In general, the peak differences among samples were affected by the encapsulating agent, but not the concentration. All films exhibited a board bands located a wavenumber of  $3270\text{ cm}^{-1}$  and  $2919\text{ cm}^{-1}$  and an intense peak at  $1025\text{ cm}^{-1}$ , which were attributed to the stretching vibrations of  $-\text{OH}$ ,  $-\text{CH}$  and  $-\text{C}-\text{O}-\text{C}$  bonds, respectively (Li et al. 2015). Strong peaks at  $1601\text{ cm}^{-1}$  and  $1409\text{ cm}^{-1}$  were detected and assigned to the asymmetric and symmetric COO stretching vibrations of the carboxylated group, respectively (Li et al. 2015). This can be attributed to the interaction between calcium ions and carboxylic group of alginate blocks and the consequent crosslinking between the different blocks of alginate (Bajdik et al. 2009; Al-Remawi 2012; Li et al. 2015).

When encapsulating agent was added new peaks were detected. Films with trehalose exhibited a new band at  $1020\text{ cm}^{-1}$ , which can be attributed to the glycosidic linkage of trehalose (Santagapita et al. 2012), and samples with  $\beta$ -cyclodextrin showed a wavenumber of  $1709\text{ cm}^{-1}$  corresponding at C=O stretch, that can indicate formation of complex inclusion (Marques 2010). Films containing Tween 20 presented three new peaks at  $2843\text{ cm}^{-1}$ ,  $1734\text{ cm}^{-1}$  and  $1339\text{ cm}^{-1}$  that corresponding at H-C-H, C=O and C-O, respectively. The bands around  $2869\text{ cm}^{-1}$  are associated with the symmetric stretching vibrations of methylene ( $-\text{CH}_2$ ), and the band at  $1730\text{ cm}^{-1}$  is originated from the C=O stretching of the ester group of the Tween molecule (Ren et al. 2012). The data described above indicated that the presence of encapsulating agents in the formulations varied interactions amount components, and therefore, different physical properties may be expected from the films.

### 3.2.4 Microstructure

In order to evaluate the structure in cross-section of the samples, SEM micrographs of films containing the highest concentration of each encapsulating agent; 0.6% trehalose, 0.25%  $\beta$ -cyclodextrin and 1% Tween 20, were showed in Figure 8a, 8b and 8c, respectively. Films with trehalose under the different concentrations studied showed a structure with a network smoother and not so porous (Fig. 8a) in comparison to films with the other encapsulating agents, especially those that contain  $\beta$ -cyclodextrin. The structure of sample with 0.25%  $\beta$ -cyclodextrin shows a rougher surface and a less homogenous network in comparison to the other films with lowest concentration. Interestingly in this sample with 0.25%  $\beta$ -cyclodextrin was possible to observe crystalline structures most likely associated to this encapsulating

agent (Steiner and Koellner 1994). The results of the image observation could confirm the discussion above on the polymer–encapsulating agent–water interactions and their effect on the molecular mobility: the films with  $\beta$ -cyclodextrin which presented more visible crystals correspond to the films with lower water relaxation times where the water molecules are less free to move in the matrix and the overall mobility in the matrix is reduced. Similar phenomenon was observed by Tao et al. (2014), in thyme freeze-dried encapsulated in  $\beta$ -cyclodextrin. Images of those powders revealed evidence of agglomeration where large particles were attracting smaller particles, and smaller clusters of particles were identified at the beginning stages of particle agglomeration. In our study, the samples with a too high Tween 20 concentration presented interactions under the measuring condition, and due to that these films were more heterogeneous and showed a cross-section where oily surface was observed. The stability of emulsions did not correlate with films microstructure indicating that interactions amount components changed when solvent was evaporated.

### **3.2.5 Encapsulation efficiency**

The addition of  $\beta$ -cyclodextrin as encapsulating agent in films with thyme oil showed the best encapsulation efficiency (Table 6), although  $\beta$ -cyclodextrin crystals were observed in the films for the highest concentration (Figure 7). Encapsulation efficiency increased as increasing concentration of encapsulating agents, except for Tween 20. As observed for optical parameters (opacity, color variation, Figure 5), Tween 20-films visually showed oily films for the highest concentration of Tween 20. This was in agreement to the low encapsulation efficiency (7.8%) obtained.

### **3.2.5 Antimicrobial activity**

The films with  $\beta$ -cyclodextrin showed the highest percentage of growth inhibition of *E. coli* comparing with trehalose and Tween 20 films (Figure 9). This could be due to the good encapsulating ability of this compound, as observed in Table 6, as it could form inclusion complexes with thymol (Ponce Cevallos et al., 2010). Also, increasing the concentration of  $\beta$ -cyclodextrin increased the percentage of inhibition of the film, which was not observed in the samples containing the other encapsulating agents. Although inhibition percentages may seem low, as desired, inhibition activity could remain with time.

## **4. Conclusions**

The three selected encapsulating agents allow preparing stable emulsions or edible films with the desired physical properties for different applications in fresh food. With natural encapsulating agents such as trehalose and  $\beta$ -cyclodextrin it was possible to obtain films as well as with Tween 20, which is important taken into account consumers preferences for natural ingredients. Both, rheological properties and stability of emulsions were suitable for coating by spray or dipping applications, especially the Tween 20 emulsion. However, as Tween 20 had the highest opacity, the film can affect the organoleptic characteristics of a fresh product. Trehalose and  $\beta$ -cyclodextrin films had less color and opacity which is an advantage in coating. Although  $\beta$ -cyclodextrin films presented crystals, they showed the best encapsulation efficiency and antimicrobial properties at initial time, however, its properties may change with time. Therefore, further research studying variation with time should be performed in the future.

### Acknowledgments

Authors acknowledgment financial support from CONICYT for Project FONDECYT REGULAR N°1131017 and fellowship awarded to author Rosa Navarro (Programa de Becas de Doctorado Nacional), ANPCYT (Argentina) for Project PICT 2013-0897, Universidad de Santiago de Chile (VRIDEI) for support of author Carla Arancibia and Programa Escala Docente Grupo AUGM (Universidad de Santiago de Chile-Universidad de Buenos Aires). Special thanks to Dr. Fernando Osorio for providing of rheometer.

### References

- Aguiar Rocha, G., Fávaro-Trindade, C., Ferreira Grosso, C. (2012). Microencapsulation of lycopene by spray drying: Characterization, stability and application of microcapsules. *Food and Bioprocess Technology*, 9, 37–42.
- Alboofetileh, M., Rezaei, M., Hosseini, H., & Abdollah, M. (2014). Antimicrobial activity of alginate/clay nanocomposite films enriched with essential oils against three common food borne pathogens. *Food Control*, 36, 1-7.
- Al-Remawi, M. (2012). Calcium Alginate Films via External Gelation. *Journal of Applied Sciences*, 12, 727-735.
- Álvarez-Cerimedo, M., Cerdeira, M., Candal, R. J., & Herrera, M. L. (2008). Microencapsulation of a low-trans fat in trehalose as affected by emulsifier type. *Journal American Oil Chemistry Society*, 85, 797–807.
- Bajdik, J., Makai, Z., Berkesi, O., Süvegh, K., Marek, T., Erős, I., & Pintye-Hódi, K. (2009). Study of the effect of lactose on the structure of sodium alginate films. *Carbohydrate Polymers*, 77, 530-535.
- Beyki, M., Zhavah, S., Tahere, S., Rahmani-Cherati, T., Abollahi, A., Bayat, M., Tabatabaei M., & Mohsenifar, A. (2014). Encapsulation of Mentha piperita essential oils in chitosan–cinnamic acid nanogel

- with enhanced antimicrobial activity against *Aspergillus flavus*. *Industrial Crops and Products*, 54, 310–319.
- Birkett, R. J. (1985). The appearance of concentrated colloid dispersions. Proceedings of the Fifth Congress of the International Colour Association. Montecarlo.
- Bonilla, J., Atarés, L., Vargas, M., & Chiralt, A. (2012). Effect of essential oils and homogenization conditions on properties of chitosan-based films. *Food Hydrocolloids*, 26, 9-16.
- Burt, S. (2004). Essential oils: their antibacterial properties and potential applications in foods—a review. *International Journal of Food Microbiology*, 94, 223 – 253.
- Cerdeira, M., Palazolo, G., Candal, R., & Herrera, M. L. (2007). Factors affecting initial retention of a microencapsulated sunflower seed oil/milk fat fraction blend. *Journal American Oil and Chemistry Society*, 84, 523–531.
- CDCP (Center for Disease Control and Prevention), & WHO (World Health Organization). (2003). Manual for the laboratory identification and antimicrobial susceptibility testing of bacterial pathogens of public health importance in the developing world. 209–214.
- Córdova, K., Tello, F., Bierhalz, A., Garnica, M. G., Martínez, H., & Grosso, C. (2015). Protein adsorption onto alginate-pectin microparticles and films produced by ionic gelation. *Journal of Food Engineering*, 154, 17–24.
- Chung, M. S., Ruan, R., Chen, P., Chung, S. H., Ahn, T. H., & Lee, K.H. (2000). Study of caking in powdered foods using nuclear magnetic resonance spectroscopy. *Journal of Food Science*, 65, 134–138.
- Del Valle, M. (2004). Cyclodextrins and their uses: a review. *Process Biochemistry*, 39, 1033–1046.
- Di Piero, P., Sorrentino, A., Mariniello, L., Giosafatto, C.V. L., & Porta R. (2011). Chitosan/whey protein film as active coating to extend Ricotta cheese shelf-life. *LWT- Food Science and Technology*, 44, 2324–2327.
- Drusch, S., Serfert, Y., Van Den Heuvel, A., & Schwarz, K. (2006). Physicochemical characterization and oxidative stability of Fish oil encapsulated in an amorphous matrix containing trehalose. *Food Research International*, 39, 807–815.
- Esparza, I., & Irache, J. M. (2011). Películas y recubrimientos comestibles como herramientas emergentes para la industria alimentaria. Editorial IMC, Madrid, España, 87-120.
- Fabra, M. J., Talens, P., & Chiralt, A. (2009). Microstructure and optical properties of sodium caseinate films containing oleic acid–beeswax mixtures. *Food Hydrocolloids*, 23, 676–683.
- Farroni, A., Matiacevich, S., Guerrero, S., Alzamora, S., & Buera, M. P. (2008). Multi-Level approach for the analysis of water effects in corn flakes. *Journal of Agricultural and Food Chemistry*, 56, 6447–6453.
- Fundo, J., Fernandes, R., Almeida, P., Carvalho, A., Feio, G., Silva, C., & Quintas, M. (2014). Molecular mobility, composition and structure analysis in glycerol plasticised chitosan films. *Food Chemistry*, 144, 2–8.
- Gibara, A., Almeida, M., dos Santos Alves, R., dos Passos-Menezes, P., Russo, M., Antunes de Souza, A., Pereira, D., & Quintans, L. (2015). Encapsulation of carvacrol, a monoterpene present in the essential oil of oregano, with  $\beta$ -cyclodextrin, improves the pharmacological response on cancer pain experimental protocols. *Chemico-Biological Interactions*, 227, 69–76.
- Giosafatto, C. V. L., Di Piero, P., Gunning, P., Mackie, A., Porta, R., & Marinello, L. (2014). Trehalose-containing hydrocolloid edible films prepared in the presence of Transglutaminase. *Biopolymers*, 101, 931-937.

- Hill, L., Gomes, C., & Taylor, T. M. (2013). Characterization of beta- cyclodextrin inclusion complexes containing essential oils (trans-cin namaldehyde, eu genol, cinnam on bark, and clove bud extracts) for antimicrobial delivery applications. *LWT - Food Science and Technology*, 51, 86-93.
- Holley, R. A. & Patel, D. (2004). Improvement in shelf-life and safety of perishable foods by plant essential oils and smoke antimicrobials. *Food Microbiology*, 22, 273-292.
- Karunasawat, K. & Anprung P. (2010). Effect of depolymerized mango pulp as a stabilizer in, oil-in-water emulsion containing sodium caseinate. *Food and Bioproducts Processing*, 88, 202-208
- Karagöz, Z., Polat, G., Kodal, B., & Candogan, K. (2010). Antimicrobial activity of soy edible films incorporated with thyme and oregano essential oils on fresh ground beef patties. *Meat Science*, 86, 283-288.
- Kester, J., & Fennema, O. (1986). Edible films and coatings: A review. *Food Technology*, 40, 47-59.
- Lacroix, M., & Vu, K. D. (2014). Edible coating and film materials: Proteins. In: Han J.H. Edition, *Innovations in Food Packaging*. Academic Press, San Diego, CA, USA, 277-294.
- Li, J., He, J., Huang, Y., Li, D., & Chen, X. (2015). Improving surface and mechanical properties of alginate films by using ethanol as a co-solvent during external gelation. *Carbohydrate polymers*, 123, 208-216.
- López, P., Sánchez, C., Batlle, R., & Nerín, C. (2007). Vapor-phase activities of cinnamon, thyme, and oregano essential oil sand key constituents against food borne microorganisms. *Journal of Agricultural and Food Chemistry*, 55, 4348 -4356.
- Luo, M. R., Cui, G., & Rigg, B. (2001). The development of the CIE 2000 colour-difference formula: CIEDE2000. *Color Research and Application*, 26, 340-350.
- Marques, H. M. C. (2010). A review on cyclodextrin encapsulation of essential oils and volatiles. *Flavour Fragrance Journal*, 25, 313-326.
- Matiacevich, S., Celis, D., Schebor, C., & Enrione, J. (2013). Physicochemical and antimicrobial properties of bovine and salmon gelatin-chitosan films. *Cyta-Journal of Food*, 11, 366-378.
- McClements, D. J. (2005). Food emulsions: Principles, practice and techniques, CRC Press, Boca Raton. Chapter 7, 269-339.
- Mchugh T. H., & Senesi, E. (2000). Apple wraps: A Novel method to improve the quality and extend the shelf life of fresh-cut apples. *Journal of Food Science*, 65, 480-485.
- Mengual, O., Meunier, G., Cayre, I., Puech, K., & Snabre, P. (1999). Characterisation of instability of concentrated dispersions by a new optical analyser: The TURBISCAN MA 1000. *Colloids and Surfaces*, 152, 111-123.
- Ortega-Toro, R., Jiménez, A., Talens, P., & Chiralt, A. (2014). Effect of the incorporation of surfactants on the physical properties of corn starch films. *Food Hydrocolloids*, 38, 66-75.
- Pedreschi, F., León, J., Mery, D., & Moyano, P. (2006). Development of a computer vision system to measure the color of potato chips. *Food Research International*, 39, 1092-1098.
- Peretto, G., Du, W., Avena-Bustillos, R., Sarreal, S. B., Sheng, S. T., Sambo, H. P., McHugh, T. H. (2014). Increasing strawberry shelf-life with carvacrol and methyl cinnamate antimicrobial vapors released from edible films. *Postharvest Biology and Technology*, 89, 11-18.
- Ponce Cevallos, P., Buera, M. P., & Elizalde, B. (2010). Encapsulation of cinnamon and thyme essential oils components (cinnamaldehyde and thymol) in beta-cyclodextrin: Effect of interactions with water on complex stability. *Journal of Food Engineering*, 99, 70-75.

- Qian, C., & McClements, D. J. (2011). Formation of nanoemulsions stabilized by model food-grade emulsifiers using high-pressure homogenization: Factors affecting particle size. *Food Hydrocolloids*, 25, 1000-1008.
- Ren, W., Tian, G., Jian, S., Gu, Z., Zhou, L., Yan, L., Jin, S., Yina, W., & Zhao, Y. (2012). Tween coated NaYF<sub>4</sub>:Yb,Er/NaYF<sub>4</sub> core/shell upconversion nanoparticles for bioimaging and drug delivery. *RSC Advances*, 2, 7037-7041.
- Ritota, M., Gianferri, R., Bucci, R., & Brosio, E. (2008). Proton NMR relaxation study of swelling and gelatinization process in rice starch–water samples. *Food Chemistry*, 110, 14–22.
- Rojas-Grau, M., Avena-Bustillos, R., Olsen, C., Friedman, M., Henika, P., Martín-Belloso, O., Pan, Z., & McHugh, T. H. (2007). Effects of plant essential oils and oil compounds on mechanical, barrier and antimicrobial properties of alginate–apple puree edible films. *Journal of Food Engineering*, 81, 634–641.
- Roudaut, C., Dacremont, & Le Meste, M. (1998). Influence of water on the crispness of cereal-based foods: acoustic, mechanical, and sensory studies. *Journal Texture and Study*, 29, 199–213.
- Santagapita, P. R., Mazzobre, M. F., & Buera, M. P. (2012). Invertase stability in alginate beads: Effect of trehalose and chitosan inclusion of drying methods. *Food Research International*, 47, 321-330.
- Solomakos, N., Govaris, A., Koidis, P., & Botsoglou, N. (2008). The antimicrobial effect of thyme essential oil, nisin and their combination against *Escherichia coli* O157:H7 in minced beef during refrigerated storage. *Meat Science*, 80, 159–166.
- Steiner, T., & Koellner, G. (1994). Crystalline P-Cyclodextrin Hydrate at Various Humidities: Fast, Continuous, and Reversible Dehydration Studied by X-ray Diffraction. *Journal of the American Chemical Society*, 116, 5122-5128.
- Tao, F., Hill, L., Peng, Y., & Gomes, C. (2014). Synthesis and characterization of  $\beta$ -cyclodextrin inclusion complexes of thymol and thyme oil for antimicrobial delivery applications. *LWT - Food Science and Technology*, 59, 247-255.
- Tapia, M. S., Rojas-Grau, M. A., Carmona, A., Rodriguez, F. J., Soliva-Fortuny, R., & Martín-Belloso, O. (2008). Use of alginate- and gellan-based coatings for improving barrier, texture and nutritional properties of fresh-cut papaya. *Food Hydrocolloids*, 22, 1493–1503.
- Villalobos, R., Chanona, J., Hernandez, P., Gutierrez, G., & Chiralt, A. (2005). Gloss and transparency of hydroxypropyl methylcellulose films containing surfactants as affected by their microstructure. *Food Hydrocolloids*, 19, 53–61.
- Yang, Y., Ming, J., & Yu, N. (2012). Color image quality assessment based on CIEDE2000. *Advances in Multimedia*, Article ID 273723, 6.
- Yuan, Y., Gao, Y., Zhao, J., & Mao, L. (2008). Characterization and stability evaluation of  $\beta$ -carotene nanoemulsions prepared by high pressure homogenization under various emulsifying conditions. *Food Research International*, 41, 61-68.
- Zúñiga, R. N., Skurtys, O., Osorio, F., Aguilera, J. M., & Pedreschi, F. (2012). Physical properties of emulsion-based hydroxypropyl methylcellulose films: Effect of their microstructure. *Carbohydrate Polymers*, 90, 1147-1158.

### Caption Figures

**Figure 1.** Flow curves of alginate-based film-forming emulsions with the lowest and the highest concentration of different encapsulating agents (○: 0.1% and ●: 0.25%  $\beta$ -cyclodextrin, ◇: 0.2% and ◆: 0.8% Trehalose, □: 0.5% and ■: 2% Tween 20).

**Figure 2.** Particle size distribution of film-forming emulsions with different type (B-CD:  $\beta$ -cyclodextrin, Tr: Trehalose and TW20: Tween 20) and concentration of encapsulating agents (◆: 0%, ▲: 0.1%B-CD or 0.2%Tr or 0.5%TW20, ●: 0.15%B-CD or 0.4%Tr or 1%TW20, ■: 0.2%B-CD or 0.6%Tr or 1.5%TW20 and ▼:0.2%B-CD or 0.6%Tr or 1.5%TW20).

**Figure 3.** Changes in percentage backscattering profiles as a function of the tube length with the storage time of film-forming emulsions containing: (a) 0,8% Trehalose, (b) 0,2%  $\beta$ -cyclodextrin, (c) 2% Tween 20 at 40°C.

**Figure 4.** Variation in backscattering (%BS) in the 30–32 mm zone of the tube monitored until 72 hours, for all film-forming emulsion stored at 40°C in quiescent conditions. The destabilization kinetics correspond to samples stabilized with 0.2%- $\beta$ -cyclodextrin ( $\beta$ -CD)(—●—), 0.2%-Trehalosa (TR)(—◆—) and 0.5%-Tween 20 (TW20)(—■—). Measuring tube length: 65 mm. Continuous lines show %BS values predicted by the first-order kinetic model used.

**Figure 5.** Difference of colour (dE2000) respect to the control samples (a) and opacity (b) of film-forming emulsions with different type and concentration of encapsulating agents (B-CD:  $\beta$ -cyclodextrin, Tr: Trehalose and TW20: Tween 20).

**Figure 6.** Relationship between  $T_{2FID}$  and temperature as a function of different agent encapsulating concentration (a) Trehalose, (b)  $\beta$ -cyclodextrin and (c) Tween 20.

**Figure 7.** SEM microstructure of films based on alginate containing different type and concentration of encapsulating agent (TR: Trehalose, TW20: Tween 20 and  $\beta$ -CD:  $\beta$ -cyclodextrin).

**Figure 8.** Inhibition of *E. coli* (express in percentage) for alginate-based films with thyme oil and different encapsulating agent concentrations ( $\beta$ -CD:  $\beta$ -cyclodextrin, TR: trehalose, TW20: Tween20) (a), and an example image of inhibition zone of films with 0.25%  $\beta$ -CD (b).

**Table 1.** Two-way ANOVA of flow parameters of film-forming emulsions based on alginate containing different type and concentration of encapsulating agents. *F* and *P* values.

	<i>Flow parameters</i> <sup>1</sup>			
	K (Pa s <sup>n</sup> )		n	
	<i>F</i> -value	<i>P</i> -value	<i>F</i> -value	<i>P</i> -value
<b>Main effects:</b>				
A: Encapsulating agent type	15.72	<0.01	16.75	<0.01
B: Encapsulating agent concentration	15.93	<0.01	13.61	<0.01
<b>Interactions:</b>				
AxB	8.86	<0.01	5.95	<0.01

<sup>1</sup> K=consistency index, n=flow index



**Table 2.** Mean values and significant differences of flow parameters for forming-film emulsions based on alginate with different type and concentration of encapsulating agents.

<i>Encapsulating agent</i>		<i>Flow parameters<sup>1</sup></i>	
Type	Concentration (%wt/wt)	K (Pa s <sup>n</sup> )	n
β-cyclodextrin	0	0.111±0.008 <sup>c</sup>	0.903±0.009 <sup>a</sup>
	0.10	0.110±0.004 <sup>c</sup>	0.901±0.003 <sup>a</sup>
	0.15	0.112±0.003 <sup>c</sup>	0.902±0.008 <sup>ab</sup>
	0.20	0.115±0.005 <sup>c</sup>	0.898±0.007 <sup>ab</sup>
	0.25	0.115±0.04 <sup>c</sup>	0.894±0.009 <sup>ab</sup>
Trehalose	0	0.111±0.008 <sup>c</sup>	0.903±0.009 <sup>a</sup>
	0.2	0.115±0.08 <sup>c</sup>	0.895±0.007 <sup>ab</sup>
	0.4	0.116±0.003 <sup>c</sup>	0.896±0.003 <sup>ab</sup>
	0.6	0.118±0.007 <sup>c</sup>	0.894±0.011 <sup>ab</sup>
	0.8	0.116±0.003 <sup>c</sup>	0.894±0.004 <sup>ab</sup>
Tween20	0	0.111±0.008 <sup>c</sup>	0.903±0.009 <sup>ab</sup>
	0.5	0.111±0.005 <sup>c</sup>	0.900±0.007 <sup>ab</sup>
	1.0	0.113±0.004 <sup>c</sup>	0.890±0.012 <sup>bc</sup>
	1.5	0.130±0.008 <sup>b</sup>	0.882±0.007 <sup>c</sup>
	2.0	0.148±0.006 <sup>a</sup>	0.855±0.007 <sup>d</sup>

<sup>a-c</sup> Means within a column with common superscripts did not differ significantly

<sup>1</sup> K=consistency index, n=flow index

**Table 3.** Mean values and standard deviation of particle size parameters for forming-film emulsions based on alginate with different type and concentration of encapsulating agents.

<i>Encapsulating agent</i>		<i>Parameters</i>	
Type	Concentration (%w/w)	Z-average size (nm)	Polydispersity Index
$\beta$ -cyclodextrin	0	3536 $\pm$ 764 <sup>a</sup>	0.46 $\pm$ 0.09 <sup>a</sup>
	0.10	2460 $\pm$ 182 <sup>bc</sup>	0.24 $\pm$ 0.05 <sup>a</sup>
	0.15	2912 $\pm$ 135 <sup>ab</sup>	0.41 $\pm$ 0.01 <sup>a</sup>
	0.20	2716 $\pm$ 354 <sup>abc</sup>	0.45 $\pm$ 0.11 <sup>a</sup>
	0.25	2680 $\pm$ 349 <sup>abc</sup>	0.39 $\pm$ 0.05 <sup>a</sup>
Trehalose	0	3536 $\pm$ 764 <sup>a</sup>	0.46 $\pm$ 0.09 <sup>a</sup>
	0.2	2812 $\pm$ 183 <sup>abc</sup>	0.51 $\pm$ 0.02 <sup>a</sup>
	0.4	2490 $\pm$ 371 <sup>bc</sup>	0.27 $\pm$ 0.02 <sup>a</sup>
	0.6	2391 $\pm$ 189 <sup>bc</sup>	0.24 $\pm$ 0.03 <sup>a</sup>
	0.8	2066 $\pm$ 192 <sup>c</sup>	0.23 $\pm$ 0.11 <sup>a</sup>
Tween20	0	3536 $\pm$ 764 <sup>a</sup>	0.46 $\pm$ 0.09 <sup>a</sup>
	0.5	2587 $\pm$ 50 <sup>bc</sup>	0.46 $\pm$ 0.07 <sup>a</sup>
	1.0	2539 $\pm$ 310 <sup>bc</sup>	0.49 $\pm$ 0.21 <sup>a</sup>
	1.5	2849 $\pm$ 21 <sup>abc</sup>	0.40 $\pm$ 0.06 <sup>a</sup>
	2.0	2739 $\pm$ 149 <sup>abc</sup>	0.43 $\pm$ 0.11 <sup>a</sup>

<sup>a-c</sup> Means within a column with common superscripts did not differ significantly

**Table 4.** Parameters of first-order kinetic equation for the BS% in the 30–32 mm zone of the tube versus ageing time for the all film-forming emulsions based on alginate, stored at 40°C, as a function of encapsulating agent type used as stabilizer.

<i>Encapsulating agent</i>		<i>Kinetic parameters for % Backscattering (BS)<sup>f</sup></i>			
Type	Concentration (% w/w)	BS <sub>e</sub>	BS <sub>0</sub> -BS <sub>e</sub>	K(s <sup>-1</sup> )	R <sup>2</sup>
$\beta$ -cyclodextrin	0.10	14.99 $\pm$ 0.02	3.61 $\pm$ 0.04	0.47 $\pm$ 0.01	0.989
	0.15	15.28 $\pm$ 0.02	1.88 $\pm$ 0.05	1.06 $\pm$ 0.19	0.857
	0.20	7.82 $\pm$ 0.39	9.47 $\pm$ 0.38	0.02 $\pm$ 0.01	0.972
	0.25	8.08 $\pm$ 0.54	9.75 $\pm$ 0.52	0.02 $\pm$ 0.002	0.970
Trehalose	0.2	14.08 $\pm$ 0.04	3.87 $\pm$ 0.05	0.07 $\pm$ 0.002	0.957
	0.4	9.41 $\pm$ 0.41	8.32 $\pm$ 0.38	0.03 $\pm$ 0.003	0.938
	0.6	12.74 $\pm$ 0.05	7.57 $\pm$ 0.09	0.18 $\pm$ 0.005	0.954
	0.8	15.48 $\pm$ 0.03	4.62 $\pm$ 0.06	0.30 $\pm$ 0.009	0.952

Tween20	0.5	12.01±0.02	4.18±0.03	0.09±0.001	0.989
	1.0	10.01±0.01	4.41±0.03	0.18±0.002	0.992
	1.5	8.44±0.00	5.26±0.01	0.08±6.13E-4	0.997
	2.0	8.97±0.03	4.72±0.06	0.63±0.03	0.956

*BSe*: backscattering percentage at the equilibrium value .

*BS0-BSe* : delta between initial and the equilibrium value of backscattering percentage

*K(s-1)*: first-order kinetic coefficient

Accepted Manuscript

**Table 5.** Two-way ANOVA of flow parameters of films based on alginate containing different type and concentration of encapsulating agents. *F* and *P* values

	$\Delta E_{2000}$		Opacity (%)	
	<i>F</i> -value	<i>P</i> -value	<i>F</i> -value	<i>P</i> -value
<b>Main effects:</b>				
A: Encapsulating agent type	126.3	<0.01	50.4	<0.01
B: Encapsulating agent concentration	52.0	<0.01	16.6	<0.01
<b>Interactions:</b>				
AxB	26.7	<0.01	13.3	<0.01

<sup>†</sup>  $\Delta E_{2000}$  = colour difference between sample with and without encapsulating agent

**Table 6.** Thermal parameters of endothermic transition associated to thyme oil (enthalpy,  $\Delta H$  and melting temperature,  $T_{\text{melting}}$ ) and encapsulation efficiency of thyme oil in films for the different encapsulating agents. Average of data and their corresponding standard deviation are reported.

<i>Encapsulating agent</i>		<i>Thermal properties</i>		<i>Encapsulation efficiency (%)</i>
Type	Concentration (% w/w)	$\Delta H$ (mJ/mg)	$T_{\text{melting}}$ (°C)	
$\beta$ -cyclodextrin	0.10	-0.64±0.06	-19.56±0.24	68.8
	0.15	-0.48±0.05	-19.72±0.23	76.6
Trehalose	0.2	-2.03±0.09	-18.68±0.59	1
	0.8	-1.75± 0.13	-18.32±0.35	14.6
Tween20	0.5	-0.98±0.03	-19.39±0.23	52.2
	2.0	-1.89±0.15	-18.99±0.12	7.8
<i>Thyme oil</i>		-2.05±0.23	-22.08±0.18	-

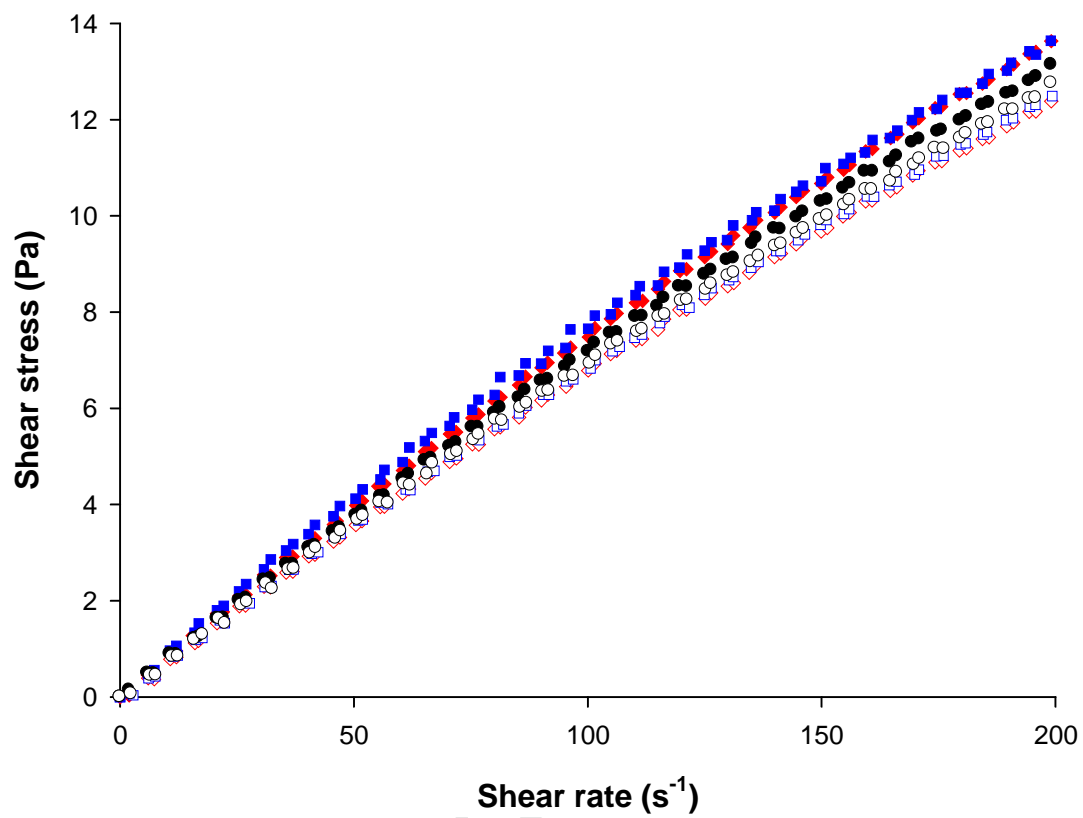


Figure 1

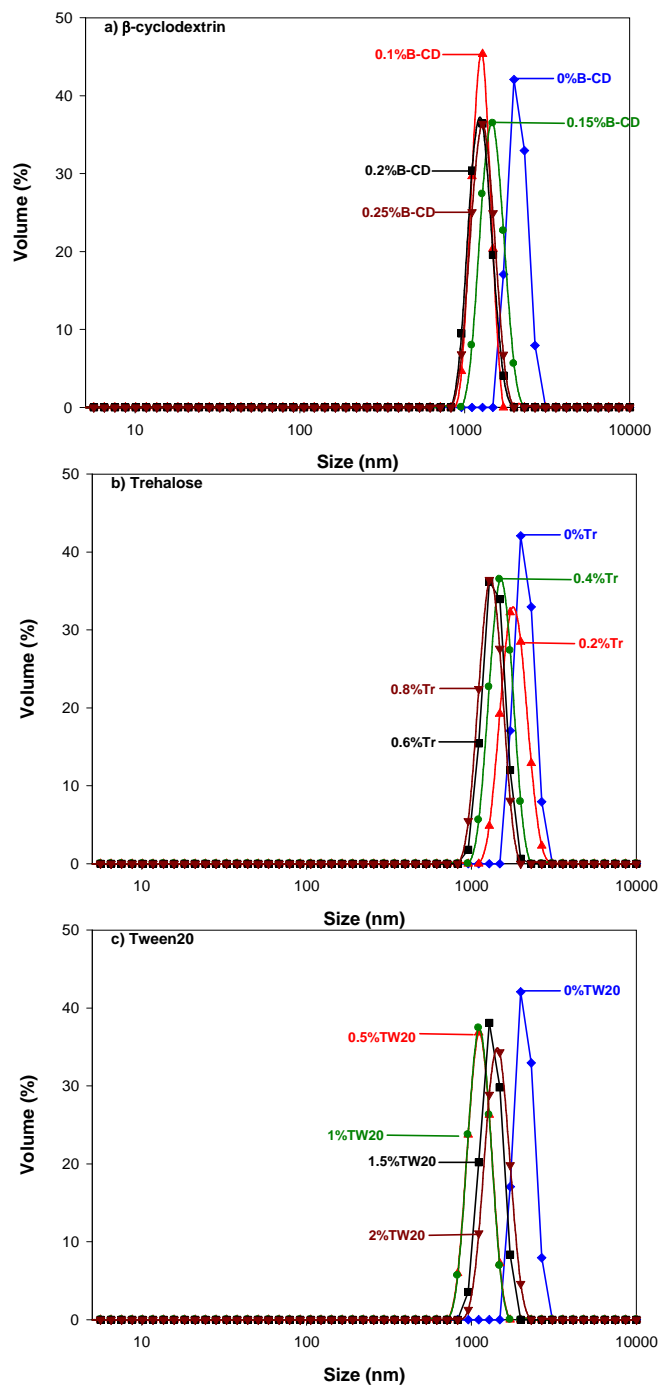


Figure 2

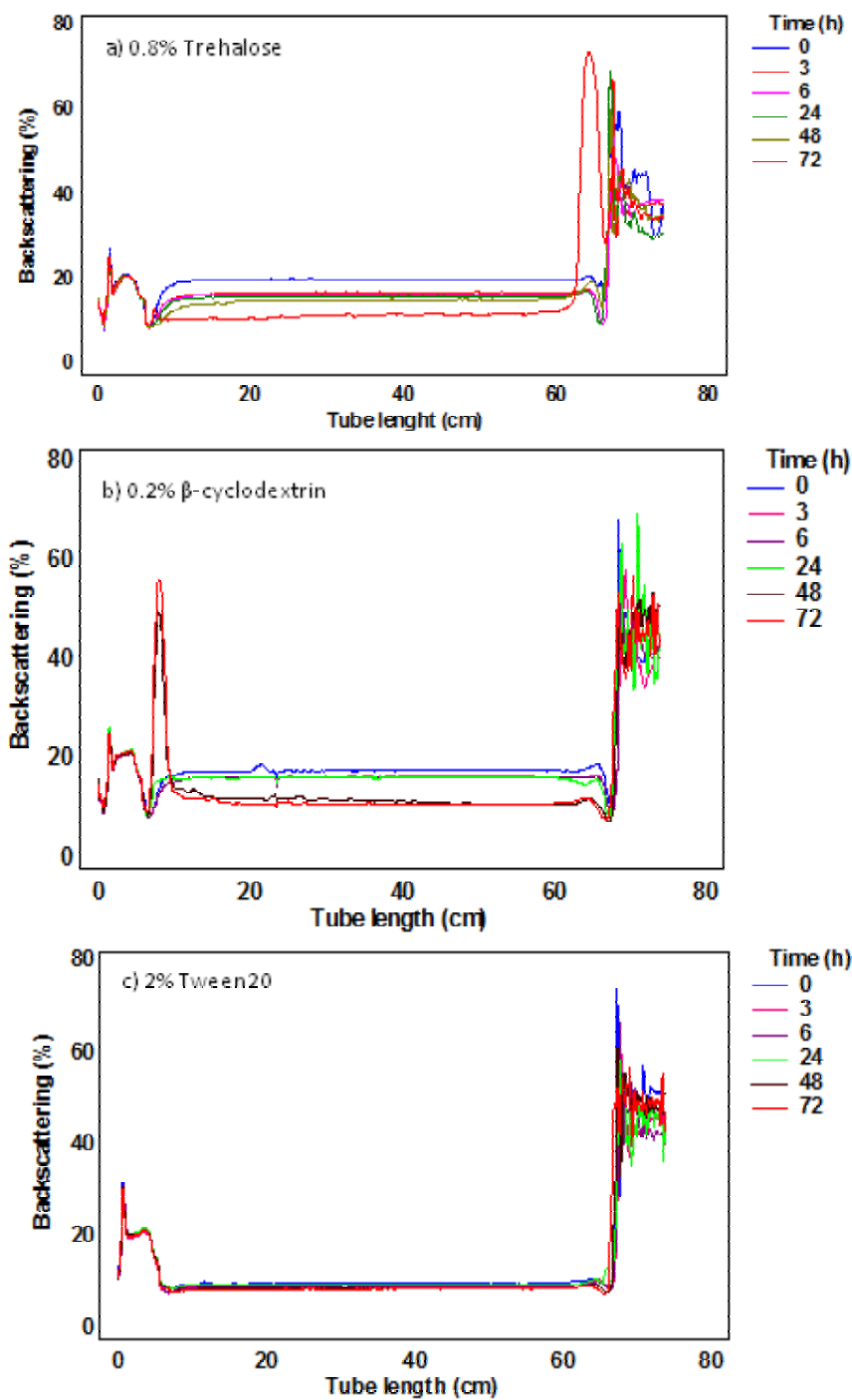


Figure 3



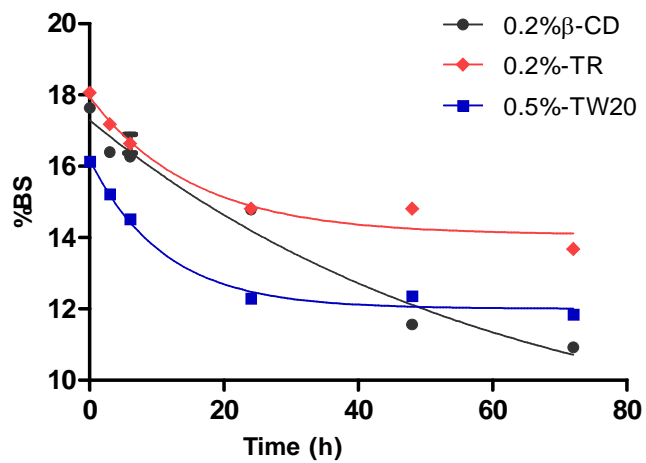


Figure 4

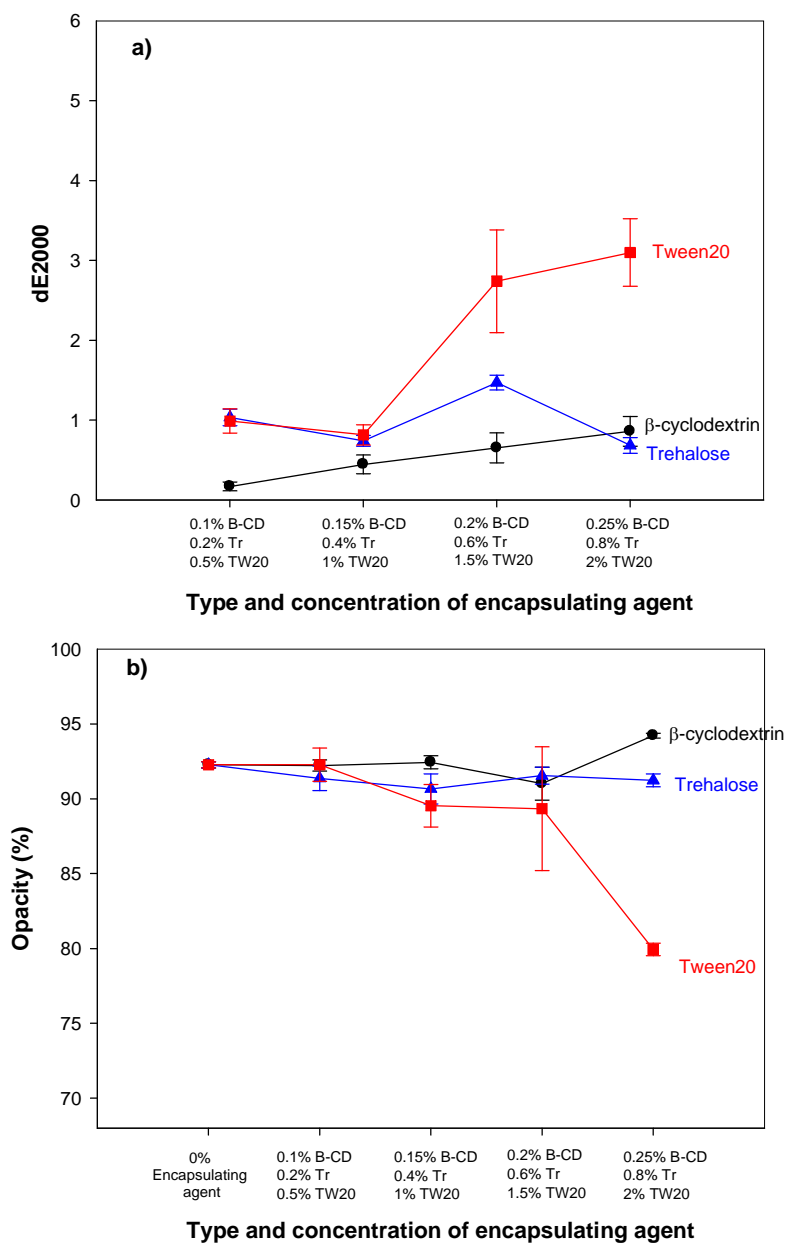


Figure 5

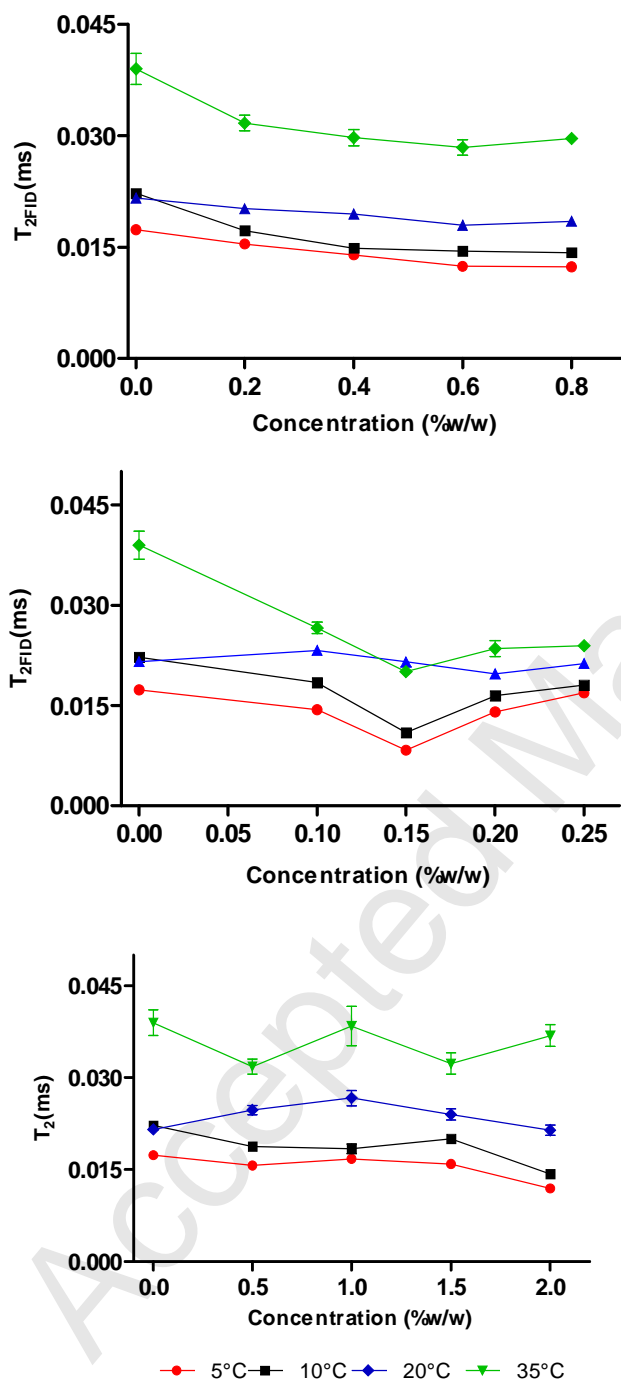
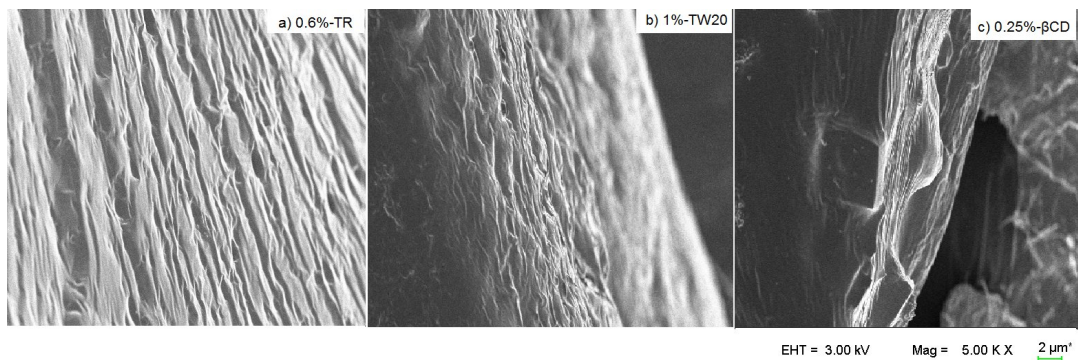
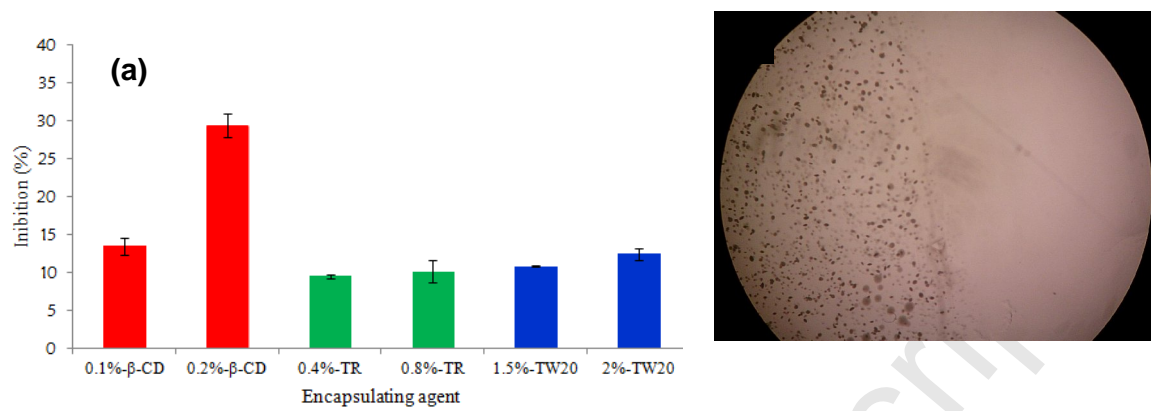


Figure 6



**Figure 7**

Accepted Manuscript

**Figure 8**

ACCEPTED MANUSCRIPT